

Original Article

Evaluation of photodynamic activity of octaethylporphyrin and vanadyl octaethylporphyrin

Joselito N. Ribeiro;¹ André R. da Silva;¹ Alessandra C. Pelegrino;² Antonio C. Tedesco;² Renato A. Jorge¹

1 Instituto de Química, Universidade Estadual de Campinas – UNICAMP, Campinas, Brazil

2 Departamento de Química, Faculdade de Filosofia Ciência e Letras, Universidade de São Paulo-USP, Ribeirão Preto, Brazil

Abstract

Objective: in this work we have investigated the photodynamic efficiency of octaethylporphyrin (OEP) and vanadyl octaethylporphyrin (VOOEP). **Methods:** this study was performed by the evaluation of photophysical parameters of these porphyrins, the photooxidation rate constants (k_p) of the biomolecules (tryptophan -Trp and bovine serum albumin - BSA) and the erythrocytes photodestruction percentage. **Results:** photophysical parameters value such as singlet oxygen quantum yield (Φ_{Δ}) and triplet state lifetime (τ_T) indicated that OEP ($\Phi_{\Delta} = 0.64 \pm 0.02$, $\tau_T = 0.91 \pm 0.02$ ms) is more efficient than VOOEP ($\Phi_{\Delta} = 0.26 \pm 0.02$, $\tau_T = 0.22 \pm 0.03$ ms). The values of $k_p/10^4 \text{ s}^{-1}$ for Trp and BSA photooxidation demonstrated that OEP (Trp= 2.80 ± 0.05 and BSA= 2.50 ± 0.1) is more efficient than VOOEP (Trp= 0.81 ± 0.08 and BSA= 0.62 ± 0.04). The photodestruction percentage of erythrocytes revealed that the photodynamic activity of OEP is more pronounced than photoactivity of VOOEP. These results indicated that differences observed in the photodynamic activity between the porphyrins could be associated with differences in their molecular structures. **Conclusion:** photophysical parameters, photooxidation of biomolecules, and photodestruction of erythrocytes clearly indicate that the vanadyl group (V=O) interferes in the photoactivity of OEP, causing a considerable reduction in its efficiency.

Key words: Photodynamic therapy. Octaethylporphyrin. Porphyrins. Hemolysis.

Introduction

Photodynamic therapy (PDT) is a promising treatment modality that employs the combination of a photosensitizer compound, molecular oxygen and visible light for cancer therapy.¹ This clinical treatment is characterized by systemic, topical, oral or parenteral administration of the photosensitizer, which is preferentially retained by tumoral tissue. In the next step of the treatment this tissue is irradiated with visible light of appropriate wavelength to excite the photosensitizer. After light absorption, a sequence of pathways takes place leading the drug to its highest excited singlet state. From the first excited singlet state, the transient species can decay by intersystem crossing to another triplet excited state, which could return to the ground state by a

phosphorescence process or transfer electrons and/or energy to ground-state oxygen, generating the superoxide anion, hydroxyl radical and (hydro)peroxides species (from a classical type I mechanism) and/or produce singlet oxygen by an energy transfer process (known as type II mechanism). These reactive oxygen species (ROS) could potentially damage biomolecules such as proteins and lipids generating other photoproducts (Figure 1). These ROS effects lead to a sequence of oxidative events and biological responses in tumoral tissue,

Correspondence

Joselito N. Ribeiro

Instituto de Química, Universidade Estadual de Campinas -UNICAMP

Cx.Postal 6154

13084-971 Campinas, Brazil

e-mail: nariber@ig.com.br

leading to cancer cell death by apoptosis and/or a necrotic process, usually associated with tumor destruction, or regression of tumor angiogenesis.^{2,3}

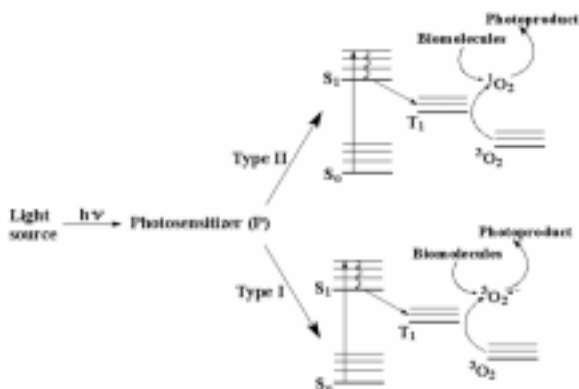


Figure 1 - Mechanisms (Type I and II) of ROS generation by combinations of light, photosensitizer (P) and ground-state oxygen ($^3\text{O}_2$). Ground-state photosensitizer (S_0) is irradiated with visible light generating excited singlet state photosensitizer (S_1). S_1 can decay by intersystem crossing to lower excited triplet state photosensitizer (T_1) then it could generate reactive oxygen species such as superoxide anion ($^3\text{O}_2^-$) (Type I) and/or singlet oxygen ($^1\text{O}_2$) (Type II)

Porphyrins are important molecules in biological systems due to their role in energy storage and oxygen transport, and they already possess several medical applications.⁴ These compounds and their derivatives are among the most useful photosensitizers for photodynamic therapy.¹ These substances constitute the first generation photosensitizers and show great potential as phototherapeutic agents for the treatment of a variety of oncological diseases.⁵ These diversified applications are at least in part a consequence of numerous approaches, which are available for the insertion of specific functional groups within the porphyrin molecule, thus imparting predetermined physicochemical properties such as hydrophobicity or hydrophilicity. Porphyrins chemical structure can be modified by introducing many different groups in axial or equatorial positions in the pyrrole ring, as well as by coordinating different metal ions with the central nitrogen atoms. These changes can strongly modulate porphyrins photophysical properties and affect their action on tumoral tissue.⁶⁻⁸

In this study we have evaluated the

photodynamic efficiency of the octaethylporphyrin (OEP) and vanadyl octaethylporphyrin (VOOEP). This work was performed through steady state (absorption, fluorescence and fluorescence quantum yield) and time resolved techniques (fluorescence lifetime, flash photolysis studies, singlet oxygen quantum yield) for OEP and VOOEP compounds (Figure 2). Furthermore, we have evaluated the influence of the vanadyl group ($\text{V}=\text{O}$) on biomolecules photooxidation (tryptophan and bovine serum albumin) and, on the photohaemolysis of human red blood cells (erythrocytes) mediated by OEP.

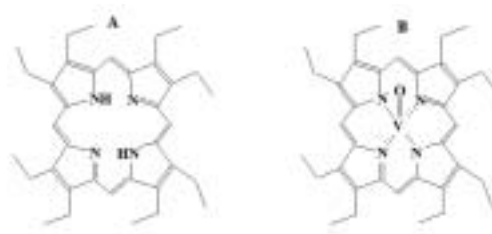


Figure 2 - Molecular structure of OEP (A) and VOOEP (B)

Material and Methods

Chemicals

VOOEP, OEP, and 5,10,15,20-tetrakis(4-N-methylpyridyl) porphyrin were purchased from Porphyrin Products, Inc. (Logan, Utah, USA). Bovine serum albumin (BSA), L-tryptophan (Trp), polyoxyethylene-sorbitan monolaurate (Tween[®]20), tetrahydrofuran (THF), methanol, and rhodamine were purchased from Sigma Chemical Company (St. Louis, USA). Chloroform, sodium chloride, dibasic sodium phosphate, and monobasic sodium phosphate were purchased from Merck (Darmstadt, Germany).

Steady state measurements

Absorption measurements were made for samples in chloroform, with a Perkin-Elmer Lambda 20 unit that was background corrected using matched quartz cuvettes, scanning over the wavelength range $\text{Abs} = 300\text{-}800\text{nm}$. Fluorescence

emission spectra were recorded using a Fluorolog 3 spectrofluorimeter from Ivon Jobin, and instrument setup file for intensity non-linearity correction of the excitation light and to adjust detector sensitivity as a function of wavelength. In fluorescence quantum yield experiments, 8 samples concentration was chosen to give absorption peak ranging 0.01-0.03 to avoid any internal filter effect. The VOOEP was excited at λ_{ex} 420nm and the OEP at 418nm with measurement of the fluorescence emission in the range λ_{em} = 500-800nm.

Fluorescence lifetime measurements

Time-correlated single-photon counting (TCSPC) was used to determine fluorescence lifetimes. This is a widely used technique and it has been extensively reviewed.⁹ The apparatus comprised a frequency-doubled mode locked Nd:YAG laser (Coherent Antares 764), which synchronously pumped a cavity-dumped dye laser (Coherent 701-3CD) with a gain medium of either Rhodamine 6G or DCM. This produced a 3.8MHz train of pulses with full width at half-maximum (FWHM) of 6 ps and an average power of 1040mW in the range 500-800nm. Fluorescence emission was collected at 90° and the emission wavelength was selected by a double-beam monochromator. A Hamamatsu 1564-UO1 microchannel plate was used to detect fluorescence emission, together with standard discriminators, time to amplitude converter (TAC) and a multi-channel analyzer (Canberra 35), giving typical instrument response times of 50 ps (FWHM). All the decays were recorded to a minimum of 20000 counts in the maximum intensity channel, and analyzed by iterative deconvolution and nonlinear least-squares fitting. The fits were validated by reduced chi-squared, visually random residuals, and autocorrelation functions.⁹

Fluorescence quantum yields

Fluorescence quantum yield was measured for each sample by the ratio method described by Eaton¹⁰ and Demas,¹¹ using 5,10,15,20-tetrakis(4-N-methylpyridyl)porphyrin in methanol as a standard, $f_r = 0.067$. Optical densities were set to 0.060 A.U. in

a chloroform medium at the wavelength of maximum absorbance and corrected fluorescence emission spectra were recorded on a Fluorog spectrofluorometer from 600 to 850nm. This technique follows that outlined by Demas and Eaton, using the equation 1:¹²

$$\phi_u = [(A_s F_u n_u^2) / (A_u F_s n_s^2)] \phi_s \quad (1)$$

where u = unknown, s = standard, ϕ = Fluorescence quantum yield, A = Absorbance, F = fluorescence area, n = solvent refractive index.

Triplet state lifetime measurements

Triplet state transient species and lifetime measurements were made using a laser flash photolysis spectrometer, which allowed the simultaneous capture of the transient absorption spectrum ($\lambda = 200-800\text{nm}$) and the transient kinetics at a single wavelength. The system is elsewhere reported in detail.¹³ Briefly, the system uses the third harmonic (355nm) of an Nd-YAG laser. Pulse length was 8ns, beam diameter incident on the sample was 6mm, and repetition rate was 10Hz. Pulse energy was typically 30mJ per pulse as measured with a Field Master power meter with L-30V head. A 400W tungsten-halogen lamp was used as probe. The lamp beam is collimated (1mm in diameter) through the sample held in a 1cm cuvette in the cell holder. The growth-decay kinetics was measured at a single wavelength using a monochromator (M300 from Bentham), and a photomultiplier (Hamamatsu, model R928P). Transient decays were averaged using a Tektronix TDS340A digital oscilloscope. Stored digitized kinetic decays were transferred to a personal computer (PC) for analysis with software supplied by Edinburgh Instruments.

Singlet oxygen measurements

The singlet oxygen measurements were based on the direct determination by luminescence measurement at 1270nm. The apparatus used in this procedure is the same as described for the triplet-excited state measurements, with small changes. The excitation laser and setup was the same. However, a German Detector operating in a nitrogen-cooled

system substitutes the photomultiplier. Signal was transferred to the same digital oscilloscope and analysis was performed with software supplied by Edinburgh. A silicon filter was used to avoid any fluorescence signal interfering in the singlet oxygen luminescence.

Photooxidation of biomolecules (Trp and BSA)

Fifty μM Trp or 10 μM BSA aqueous solutions were prepared in phosphate buffer saline (PBS: 0.15M NaCl, 1.9mM NaH_2PO_4 , 8.1mM Na_2HPO_4 , pH 7.4) containing 0.1% (v:v) Tween[®] 20, 2% (v:v) THF, and 5 μM OEP or VOOEP. These solutions were saturated with oxygen and irradiated with a mercury lamp (using a filter for 400-600nm) for 50 minutes. The fluorescence of biomolecules was monitored at 10-minute intervals using a Perkin Elmer LS55 luminescence spectrometer to determine the photooxidation rate constant for Trp and BSA. Biomolecule photooxidation occurs obeying a first-order kinetics, as determined in our laboratory. Therefore, biomolecular photooxidation rate constant was calculated by the equation: $\ln(F_0/F) = k_p \cdot t$ (F_0 = initial fluorescence and F = fluorescence at time t in 360nm for Trp and 330nm for BSA, k_p = photooxidation rate constant).

Photohaemolysis of erythrocytes

Human blood samples were obtained from the Hospital of Campinas State University (Campinas, Brazil) through the courtesy of Dilmara Lopes Vicentim, Michele Goulart, and Heloisa Cristina Acosta. The blood was stored in heparinized tubes (0.2mg of heparin/2mL of blood) at 4°C and used within 2 days. Just before the experiment, the blood was centrifuged (3000rpm for 10 minutes), and the buffy coat and plasma were discarded. A solution of 0.5% erythrocytes was prepared in PBS containing 0.05% (v:v) Tween[®] 20, 0.2% (v:v) THF, and 5 μM OEP or VOOEP. This solution was saturated with oxygen and irradiated with a mercury lamp (using a filter for 400-600nm) for 60 minutes. The

photohaemolysis of erythrocytes was determined at 10-minute intervals by withdrawing a sample (800 μL), which was immediately centrifuged, the supernatant (500 μL) being diluted to 1mL with PBS. After 20 minutes the photohaemolysis was determined by absorbance readings (at 540nm) of haemoglobin (using a Hewlett Packard 8453 spectrophotometer), present in supernatant, released from the photodamaged erythrocyte. The percentage of photohaemolysis due to added photosensitizer is defined as $100(A_1 - A_2)/A_\alpha$, where, for a given time, A_1 is the absorbance for the test sample and A_2 is the absorbance for the control (i.e. without photosensitizer); A_α is the absorbance for total haemolysis, which was determined after lysis (using a Model 8890R-MT ultrasonic bath, Cole-Parmer, Vernon Hills, USA, for 15 minutes) of 0.5% erythrocytes in distilled water.

Results

Spectra of the porphyrins

Absorption spectra of OEP and VOOEP showed the presence of the Soret band between 350 to 440 nm (Figure 3). Figure 4 shows the fluorescence emission spectra with maximum emissions located at 622 nm for OEP and at 716 nm for VOOEP. The maximum intensities of the fluorescence and absorption bands of OEP and VOOEP are shown in Table 1.

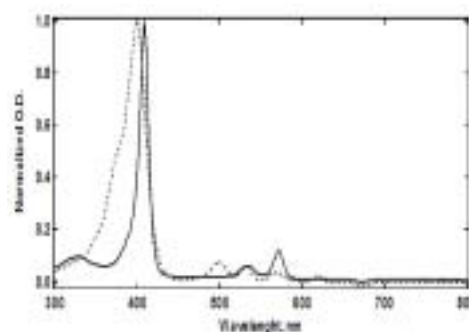


Figure 3 - Normalized absorption spectra of VOOEP (5 μM in chloroform —) and OEP (5 μM in chloroform —)

Table 1 - Photophysical parameters of VOOEP and OEP (5 μ M in chloroform). I = fluorescence maximum emission, τ_T = triplet state lifetime, ϕ_f = fluorescence quantum yield, and Φ_{Δ} = singlet oxygen quantum yield.

Photosensitizer	Absorption Q-bands and Soret band/nm	I/nm	τ_T air-equilibrated/ μ m	τ_f air-equilibrated/ns	ϕ_f	Φ_{Δ}
OEP	398, 496, 532, 566 and 620	622	0.91+0.002	10.2_1.0	0.8+0.001	0.64+0.002
VOEP	408, 532	716	0.22+0.003	-----	0.021+0.01	0.26+0.002

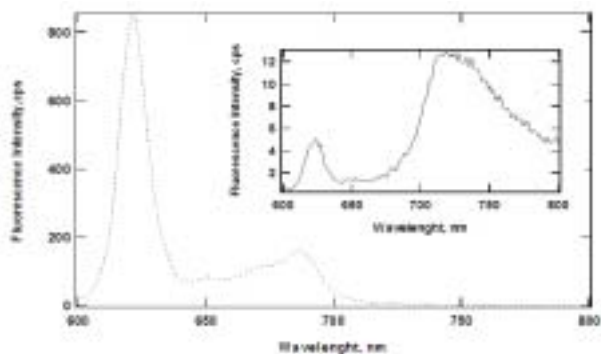


Figure 4 - Fluorescence emission spectrum of OEP (5 μ M) in chloroform, with fixed λ_{Ex} = 418nm (—). Inset: Fluorescence emission of VOOEP (23 μ M) in chloroform (---) with λ_{Ex} =420nm

Fluorescence quantum yields, lifetime and triplet state lifetime

The results of fluorescence quantum yield, triplet state lifetime and other photophysical parameters of OEP and VOOEP are shown in Table 1.

The OEP transient spectra present a maximum at 460nm with a higher triplet lifetime than VOOEP (Figure 5). The OEP transient has a better absorption in the region from 200 to 800nm, compared to VOOEP.

The singlet oxygen quantum yields measured by luminescence emission at 1270nm for VOOEP and OEP are presented in Table 1

These results provide evidence that the presence of the vanadyl group reduces the values of photophysical parameters of OEP.

Photooxidation of biomolecules

The fluorescence intensity of Trp (Figure 6) and BSA (Figure 7) has decreased in the presence of OEP and VOOEP. This event occurred according to a first-order kinetics, as determined in our laboratory. Moreover the fluorescence spectra and the values of the photooxidation rate constant (Table 2) demonstrate that VOOEP is less effective than OEP in photooxidation of Trp and BSA.

Photohaemolysis of erythrocytes

The photohaemolysis of erythrocytes mediated by OEP is more evident than by VOOEP (Figure 8) indicating that the vanadyl group decreased the efficiency of OEP.

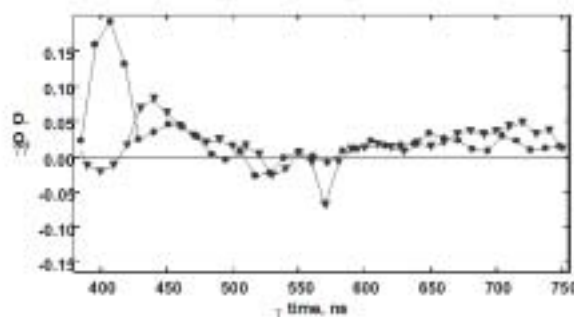


Figure 5 - Transient absorbance spectrum of dyes in chloroform after excitation at a wavelength of 355nm (30mJ per pulse). Triplet state for VOOEP showing the characteristic absorption at 460nm (\blacktriangledown). Spectrum of OEP showing a longer lived triplet excited state with a maximum 407nm (\bullet)

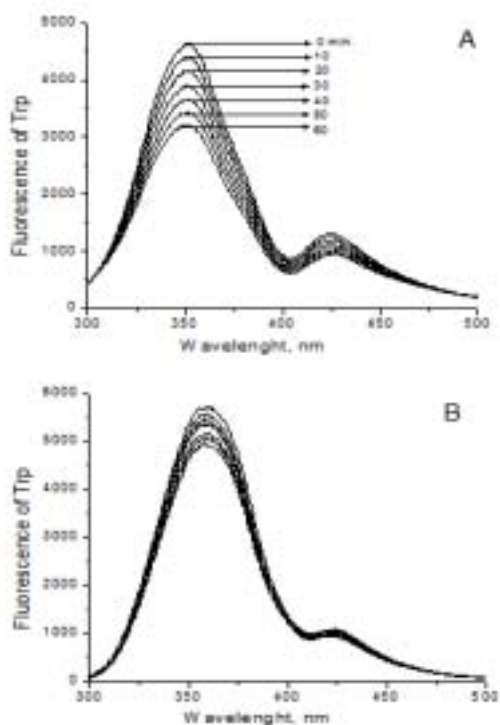


Figure 6 - Decrease of fluorescence spectra intensity of Trp in the presence of light, oxygen, and OEP (A) or VOOEP (B)

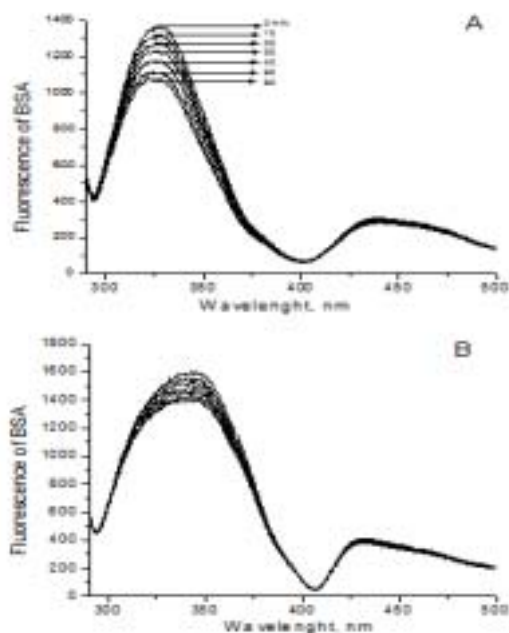


Figure 7 - Decrease of fluorescence spectra intensity of BSA in the presence of light, oxygen, and OEP (A) or VOOEP (B)

Table 2 - Values of k_p for photooxidation of Trp and BSA mediated by OEP and VOOEP

Photosensitizer	k_p for Trp / $10^{-4}s^{-1}$	k_p for BSA / $10^{-5}s^{-1}$
OEP	1.06 ± 0.03	7.20 ± 0.03
VOOEP	0.40 ± 0.05	3.2 ± 0.2

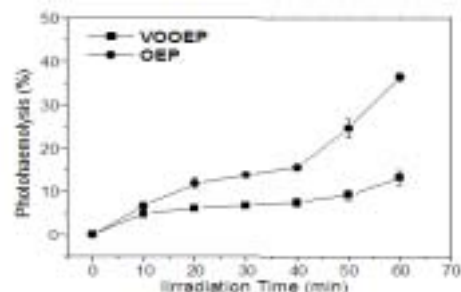


Figure 8 - Percentage of erythrocyte photohaemolysis mediated by OEP and VOOEP

Discussion

Spectra of the porphyrins

Absorption spectra of the dye in chloroform solution are characteristic of non-aggregated species in the range of concentration studied (from 5 to $20\mu\text{M}$) (Figure 3). Both compounds (OEP and VOOEP) showed the classical presence of the Soret band (between 350 to 440nm) that is related to the transition from orbital a_{1u} to degenerated orbital e_g (referring to vibronic progression $v_o \rightarrow v_o$) and a group of absorption Q-bands that are related to the transition from orbital a_{2u} to degenerated orbital e_g . It is observed that OEP, in contrast to VOOEP, has four Q-bands, while VOOEP has two Q-bands. Non-metalloporphyrins as OEP present distortions in the basic structure of the molecule, i.e., in the pyrrol rings, causing a difference of 25 to 29kJ mol^{-1} between energy levels, and consequently increased Q-band number.¹⁴

The dipoles of the non-metalloporphyrins (OEP) related to transitions $\pi \rightarrow \pi^*$ are not equivalent in the x and y directions, due to distortions in the ring structure of the molecule. Therefore, the Q_x -band ($v_o \rightarrow v_o$) cannot be convoluted with the Q_y -band ($v_o \rightarrow v_o$), nor can the Q_x -band ($v_o \rightarrow v_1$) be

convoluted with the Q_y -band ($\nu_o \rightarrow \nu_1$), resulting in four Q-bands. The first Q-band at 498 nm (highest energy) is identified as IV-band ($Q_x, \nu_o \rightarrow \nu_1$), the second band at 532nm is identified as III-band ($Q_y, \nu_o \rightarrow \nu_o$), the third band at 566nm as II-band ($Q_y, \nu_o \rightarrow \nu_1$) and the fourth band at 620nm as I-band ($Q_y, \nu_o \rightarrow \nu_o$). In metalloporphyrins (VOOEP) with D_{4h} symmetry (planar), transitions $\pi \rightarrow \pi^*$ present equivalent dipoles in the x and y directions. Therefore, only one Q_a -band referring to the transition $\nu_o \rightarrow \nu_o$ can be observed in VOOEP at 572nm and one Q_b -band referring to the transition $\nu_o \rightarrow \nu_1$ can be observed at 532nm, resulting into two Q-bands.¹⁴ As shown in Figure 4, the fluorescence emission spectra show maximum emissions located at 622nm for OEP and at 716nm for VOOEP, thus corroborating with these porphyrins characteristics. The maximum intensities of the fluorescence and absorption bands of OEP and VOOEP are shown in Table 1.

Fluorescence quantum yields, lifetime and triplet state lifetime

The results of fluorescence quantum yield, triplet state lifetime and other photophysical parameters of OEP and VOOEP are shown in Table 1.

The lower value of the fluorescence quantum yield ($\phi_f = 0.021$ for VOOEP) is in agreement with the emission spectra shown in the insert of Figure 4, where the dye must be used at a higher concentration (23 μ M) to detect some fluorescence signal. The fluorescence lifetime of VOOEP could not be detected at normal conditions mainly because it was in the picosecond range. For the OEP, however, a value of $\phi_f = 0.814$ is consistent with this class of compounds. Fluorescence signal (Figure 4) and fluorescence lifetime (10ns) complete the analysis of the behavior of this class of dye in their singlet excited state. These results permit to conclude that photoexcited OEP does not significantly return to the ground state via radiationless pathways. With this higher fluorescence quantum yield, we could consider that most of the OEP molecules return to the ground state by fluorescence emission. Therefore, OEP can be considered a good substance to use in

photodiagnostic procedures. The same is not true, however, for VOOEP compound, which presents a lower fluorescence quantum yield. The presence of the vanadyl group causes a decrease of the OEP fluorescence quantum yield.

The OEP transient spectra present a maximum at 460 nm with a triplet lifetime higher than those of VOOEP. These maxima agree well with the excited triplet state of many porphyrins derivatives.¹² The OEP transient has better absorption in the region from 200 to 800nm, compared to VOOEP (Figure 5).

The dye OEP has a lived triplet lifetime (0.91ms) longer than VOOEP (0.22ms) in an air-equilibrated solution (Table 1). This is an evidence that the absence of the vanadyl group prolongs the triplet state lifetime of OEP. Because of its longer triplet lifetime, OEP has a good possibility of interacting with ground-state oxygen, generating more reactive oxygen species, than VOOEP, allowing the dye to work more efficiently as a photosensitizer for PDT protocols (Type I or Type II reaction).

The singlet oxygen quantum yields measured by luminescence emission at 1270nm for VOOEP and OEP are presented in Table 1. The value found for OEP ($\Phi_\Delta = 0.64$) is 3 times higher than the value for VOOEP ($\Phi_\Delta = 0.26$), which is in agreement with other photophysical properties measured. These results prove that the presence of the vanadyl group reduces the photodynamic action of the octaethylporphyrin, consonant with the photooxidation studies described in the next section.

Photooxidation of biomolecules

For most photosensitizers the PDT effect is mediated by type II reactions, which involve singlet oxygen production. The key role played by this reactive oxygen species in PDT damage is well documented. This reactive specie is very efficient in producing oxidized forms of biomolecules, thus initiating most types of PDT damage.¹⁵ Singlet oxygen can react with unsaturated lipids and α -aminoacid residues, especially tryptophan.¹⁶ This aminoacid represents a suitable substrate for testing the efficiency of photosensitizing agents since it is well photooxidized both by type I and type II reaction

mechanisms.¹⁷

Additionally BSA protein can also be used for testing the efficiency of photosensitizing agents. Porphyrin-sensitized photooxidation of BSA provides oxidation of the protein, at least, in two different specific sites: the Cys-34 residue, giving rise to a thyl radical; and one or both of the tryptophan residues (Trp-134 and Trp-214), resulting in the formation of tertiary carbon-centered radicals and disruption of the tryptophan ring system.¹⁸ The photooxidation of Trp and BSA mediated by photosensitizers can be measured by decreases in the biomolecular fluorescence over time since fluorescence intensity and concentration are proportional. In this experiment, we have observed that the fluorescence intensity of Trp (Figure 6) and BSA (Figure 7) decreased in the presence of OEP and VOOEP. This event occurred according to a first-order kinetics, as determined in our laboratory. Moreover, the fluorescence spectra and the values of the photooxidation rate constant (Table 2) demonstrate that VOOEP is less effective than OEP in photooxidation of Trp and BSA suggesting that, under our experimental conditions, ROS production mediated by OEP is less efficient when the vanadyl group is present. These results of biomolecular photooxidation are in agreement with the longer triplet state lifetime and the better transient absorption of OEP. Probably, the vanadyl group provokes an increase of excited photosensitizer decline by a non-radioactive process causing decreased triplet state lifetime and fluorescence quantum yield of OEP, and consequently reducing its photodynamic efficiency.

Photohaemolysis of erythrocytes

Photohaemolysis is a term used to describe the light-induced rupture of erythrocyte membrane, and it is conveniently monitored by measuring the release of haemoglobin into the medium.¹⁹ This process can be mediated by porphyrins, oxygen, and light resulting in singlet oxygen production. Reactive oxygen species react with constituents of biological membranes leading to alteration of cell permeability and possible cytolysis.¹⁵

Erythrocytes Photohaemolysis can be used to evaluate the efficiency of photodynamic activity of photosensitizers.¹⁹ In our experiment the results of photohaemolysis demonstrated that OEP is more efficient than VOOEP (Figure 8). These results are consistent with photooxidation of biomolecules and photophysical parameters, indicating that the vanadyl group decreased the efficiency of OEP.

Conclusion

It is conceivable that differences observed in the photodynamic activity between photosensitizers could be associated with differences in their molecular structures. This is certainly the case of OEP. The photophysical parameters, photooxidation of biomolecules, and photohaemolysis of erythrocytes identified clearly that the vanadyl group interferes in the photodynamic activity of this photosensitizer, leading to a reduction in its photodynamic efficiency. Furthermore, the results of this study demonstrated that OEP is a promising photosensitizer compound, which can be tested for use in photodynamic therapy.

Acknowledgements

The authors would like to acknowledge financial support from the Coordenação de Aperfeiçoamento de Pessoal de Nível Superior (CAPES), the Conselho Nacional de Desenvolvimento Científico e Tecnológico, and the Fundação de Amparo a Pesquisa do Estado de São Paulo (FAPESP).

References

- Huang Z. A review of progress in clinical photodynamic therapy. *Technol Cancer Res Treat* 2005;4:283-93.
- Plaetzer K, Kiesslich T, Oberdanner CB, Krammer B. Apoptosis following photodynamic tumor therapy: Induction, mechanisms and detection. *Curr Pharma Des* 2005;11:1151-65.
- Ribeiro JN, Silva AR, Jorge RA. Involvement of mitochondria in apoptosis of cancer cells induced by photodynamic therapy. *J Bras Patol Med Lab* 2004;40:385-92.
- Ebeid EM, Habib AM, Abdel-Kader MH, Yousef AB, Guilard R. Spectroscopic and stability characteristics of ga-tetraphenyl porphyrin chloride and ge-tetra(para-methyl-phenyl) porphyrin chloride and sn-tetra(para-methyl-phenyl) porphyrin chlorides. *Spectrochim Acta* 1988;44:127-30.
- Levy JG, Obochi M. New applications in photodynamic therapy introduction. *Photochem Photobiol* 1996;64:737-9.
- Reddi E, Jori G. Steady-state and time-resolved spectroscopic studies of photodynamic sensitizers - porphyrins and phthalocyanines. *Rev Chem Intermediat* 1988;10:241-268.

- Bock G, Harnett S. Photosensitizing Compounds: their Chemistry, Biology and Clinical Use. Chichester: Wiley; 1989.
- Chakrabart AN, Molnar J, Dastidar SG, Motohashi N. Non Antibiotics. New Delhi: Niscon; 1998.
- Oldham TC, Phillips D. Triplet-state photophysics of aluminium phthalocyanine sensitizer in murine cancer cells. J Photochem Photobiol B 2000;55:16-9.
- Eaton FD. Study of fluorescence lifetime. Pure Appl Chem 1988;60:1107-14.
- Demas JN. Excited State Lifetime Measurements, New York: Academic Press; 1983.
- Foley MSC, Beeby A, Parker AW, Bishop SM, Phillips D. Excited triplet state photophysics of the sulphonated aluminium phthalocyanines bound to human serum albumin. J Photochem Photobiol B 1997;38:10-7.
- Tedesco AC, Rotta JCR, Lunardi CN. Synthesis, photophysical and photochemical aspects of phthalocyanines for photodynamic therapy. Cur Org Chem 2003;7:187-96.
- Gouterman M. Spectra of porphyrins. J Mol Spectrosc 1961;6:138-63.
- Via LD, Magno SM. Photochemotherapy in the treatment of cancer. Curr Med Chem 2001;8:1405-18.
- Bonnett R. Photosensitizers of the porphyrin and phthalocyanines series for photodynamic therapy. Chem Soc Rev 1995;24:19-33.
- Segalla A, Borsarelli CD, Braslavsky SE, Spikes JD, Roncucci G, Dei D, Chiti G, Jori G, Reddi E. Photophysical, photochemical and antibacterial photosensitizing properties of a novel octacationic Zn(II)-phthalocyanine. Photochem Photobiol Sci 2002;1:641-8.
- Silvester JA, Timmins GS, Davies MJ. Photodynamically generated bovine serum albumin radicals: Evidence for damage transfer and oxidation at cysteine and tryptophan residues. Free Radical Biol Med 1998;24:754-66.
- Paolis A, Chandra S, Charalambides AA, Bonnett R, Magnus IA. The effect on photohemolysis of variation in the structure of the porphyrin photosensitizer. Biochem J 1985;226:757-66.

Curso Básico Anual de Cancerologia do Hospital do Câncer

MÓDULOS:

- 1 - Metodologia e Estatística
- 2 - Epidemiologia e Biologia Molecular
- 3 - Diagnóstico em Oncologia
- 4 - Estadiamento e Bases Terapêuticas da Oncologia
- 5 - Cuidados Paliativos, Ética Médica e Emergências Oncológicas
- 6 - Neoplasias do Trato Aero-Digestivo Superior
- 7 - Câncer de Mama
- 8 - Neoplasias do Trato Digestivo Alto: Esôfago e Estômago
- 9 - Câncer Colorretal
- 10 - Câncer de Próstata e Câncer de Colo de Útero
- 11 - Melanoma e Onco-Hematologia

2006
de 11 fevereiro
a 2 de dezembro

Carga Horária:
Um Sábado por mês
das 8 às 12hs.
Por módulo: 04 horas
Total: 44 horas

Coordenação:
Dr. Samuel Aguiar Junior
Prof. Ademair Lopes
Dr. Francisco Ricardo Guadalupe Coelho

Público Alvo:
Alunos de Graduação, Pós-Graduação
e Profissionais da Área da Saúde

Informações e inscrições:
Centro de Estudos do Hospital do Câncer
Tel./Fax: (11) 2169-5078 - 2169-5098
e-mail: centrodeestudos@hcancer.org.br
site: hcancer.org.br

Apoio:

Realização:

HOSPITAL DO CANCER
CENTRO DE ESTUDOS

Local: Auditório Sen. José Ermirio de Moraes
R. Yrmandiré 764
Liberdade - São Paulo - SP